



**HAL**  
open science

## COMPUTATION OF MINIMAL SURFACES

H. Terrones

► **To cite this version:**

H. Terrones. COMPUTATION OF MINIMAL SURFACES. Journal de Physique Colloques, 1990, 51 (C7), pp.C7-345-C7-362. 10.1051/jphyscol:1990735 . jpa-00231134

**HAL Id: jpa-00231134**

**<https://hal.science/jpa-00231134>**

Submitted on 4 Feb 2008

**HAL** is a multi-disciplinary open access archive for the deposit and dissemination of scientific research documents, whether they are published or not. The documents may come from teaching and research institutions in France or abroad, or from public or private research centers.

L'archive ouverte pluridisciplinaire **HAL**, est destinée au dépôt et à la diffusion de documents scientifiques de niveau recherche, publiés ou non, émanant des établissements d'enseignement et de recherche français ou étrangers, des laboratoires publics ou privés.

## COMPUTATION OF MINIMAL SURFACES

H. TERRONES

*Department of Crystallography, Birkbeck College, University of London,  
Malet Street, GB-London WC1E 7HX, Great-Britain*

## Abstract

The study of minimal surfaces is related to different areas of science like Mathematics, Physics, Chemistry and Biology. Therefore, it is important to make more accessible concepts which in the past were used only by mathematicians. These concepts are analysed here in order to compute some minimal surfaces by solving the Weierstrass equations. A collected list of Weierstrass functions is given. Knowing these functions we can get important characteristics of a minimal surface like the metric, the unit normal vectors and the Gaussian curvature.

## 1 Introduction

The study of Minimal Surfaces (MS) is not a new field. Since long time ago, people have been attracted by the shapes and properties of soap films. There is evidence that Leonardo da Vinci was interested in this topic [15],[18] although, the study became more formal in the last century when the Belgian physicist Joseph Antoine Ferdinand Plateau (1801-1883) published in 1873 a large part of his observations and theoretical points of view in the "Traité de Statique Expérimentale et Théorique des Liquides Soumis aux Seules Forces Moléculaires [17](Experimental and Theoretical Statics of Liquids Subjected Solely to Molecular Forces). In this work he illustrated that a minimal surface can be obtained as a soap film by dipping a closed wire into soapy water. These experiments suggested the problem of finding a MS contained by a boundary (the Plateau problem). During that time mathematicians like Schwarz (who discovered the D,P,H,T and CLP triply periodic minimal surfaces), Riemann, Weierstrass and others were attracted by the problem. In 1930 the American mathematician Jesse Douglas [4] and the Hungarian Tibor Radó [20] gave some general solutions to the Plateau problem under certain conditions.

Due to the properties of MS, this field has been extended to other areas different from Mathematics, like Chemistry, Biology and Physics. For example, MS have been used as a model of liquid crystal phases [22], to describe structures of lipid bilayers [7], to characterise inorganic structures [2], [13], [14], to elucidate properties of surfactants and co-polymers [1] etc. Since the research on MS is interdisciplinary, it is important to make accessible some mathematical concepts which are relevant for the computation of these surfaces. The

computation of MS plays an important role because permits us to visualize and analyse its properties. In the first section of this work, the Weierstrass equations in different but equivalent forms are given. These equations allow us to compute the coordinates  $x, y, z$  and also important parameters for characterising the surface like the metric, the normal vectors and the Gaussian curvature. In the second section, Weierstrass functions (functions which compose the Weierstrass equations) for some examples of non-periodic, singly periodic and doubly periodic MS are studied. In addition, the Bonnet transformation and its importance as a useful tool for generating new MS is analysed. Finally, the third section is devoted to triply periodic minimal surfaces (TPMS). The computation of TPMS using Weierstrass functions obtained by an algorithm developed by Lidin and Hyde [11] is studied. A list of the Weierstrass functions for TPMS is provided.

## 2 Minimal Surfaces and the Weierstrass Equations

A minimal surface is defined as a surface with zero mean curvature ( $H=0$ ) at every point. The mean curvature is the average of the two principal curvatures in the surface [23]. This means that a MS bends equally to both sides at every point. In other words, each point is a symmetric saddle. Since in most of the cases it is difficult, and sometimes not possible, to find functions  $f(x, y, z) = 0$  for a M.S. in Cartesian 3-space as in the catenoid or the helicoid, we have to use a method which enable us to calculate these surfaces. In 1866 the German mathematician K. Weierstrass published a set of equations for obtaining the coordinates  $(x, y, z)$  of a minimal surface [24]. These equations can be written in the following equivalent forms:

$$\begin{aligned} x &= \operatorname{Re} \int_{\rho_0}^{\rho_1} (P^2(\rho) - Q^2(\rho)) d\rho \\ y &= \operatorname{Re} \int_{\rho_0}^{\rho_1} i(P^2(\rho)^2 + Q^2(\rho)) d\rho \\ z &= \operatorname{Re} \int_{\rho_0}^{\rho_1} 2P(\rho)Q(\rho) d\rho \end{aligned} \quad (1)$$

Where  $\rho = \rho_a + i \rho_b$ .

$$\begin{aligned} x &= \operatorname{Re} \int_{\omega_0}^{\omega_1} (1 - \omega^2) R(\omega) d\omega \\ y &= \operatorname{Re} \int_{\omega_0}^{\omega_1} i(1 + \omega^2) R(\omega) d\omega \\ z &= \operatorname{Re} \int_{\omega_0}^{\omega_1} 2R(\omega)\omega d\omega \end{aligned} \quad (2)$$

Where  $\omega = \omega_a + i \omega_b$ .

$$\begin{aligned} x &= \operatorname{Re} \int_{\tau_0}^{\tau_1} \frac{1}{2} F(\tau)(1 - G^2(\tau)) d\tau \\ y &= \operatorname{Re} \int_{\tau_0}^{\tau_1} \frac{1}{2} i F(\tau)(1 + G^2(\tau)) d\tau \\ z &= \operatorname{Re} \int_{\tau_0}^{\tau_1} F(\tau)G(\tau) d\tau \end{aligned} \quad (3)$$

Where  $\tau = \tau_a + i \tau_b$  and  $i = \sqrt{-1}$ .

The Weierstrass equations guarantee that the surface obtained is a MS and this comes from the fact that the MS  $\vec{r}(x(u, v), y(u, v), z(u, v))$  satisfies Laplace's equation with respect to the isothermal parameters "u" and "v" [9], in other words

$$\frac{\partial^2 \vec{r}(u, v)}{\partial u^2} + \frac{\partial^2 \vec{r}(u, v)}{\partial v^2} = 0 \quad (4)$$

Therefore,  $\vec{r}(u, v)$  is harmonic and can be expressed as the real part of an analytical function [3].

Knowing the complex functions which compose the Weierstrass equations, we can derive the expressions for the metric, the unit normal vectors (Gauss map) and the Gaussian curvature. These parameters are important for characterising the surface.

For equations (1) the coefficients of the metric or first fundamental form  $g_{11}$ ,  $g_{12}$  and  $g_{22}$  can be written as

$$g_{11} = \frac{\partial \vec{r}(u, v)}{\partial u} \cdot \frac{\partial \vec{r}(u, v)}{\partial u} = \vec{r}_1 \cdot \vec{r}_1 = (|P|^2 + |Q|^2)^2 \quad (5)$$

$g_{22} = g_{11}$  since "u" and "v" are isothermal parameters and  $g_{12} = 0$  because isothermal parameters are orthogonal [9].

The unit normal vectors (Gauss map) are given by

$$\vec{N} = \frac{\vec{r}_1 \times \vec{r}_2}{|\vec{r}_1 \times \vec{r}_2|} = \frac{1}{|P|^2 + |Q|^2} [2 \operatorname{Re}[P Q^*], 2 \operatorname{Im}[P Q^*], |Q|^2 - |P|^2] \quad (6)$$

Where  $Q^*$  is the complex conjugate of  $Q$ , the symbol  $||$  denotes the modulus of a function of complex variable, and  $\operatorname{Re}[\ ]$ ,  $\operatorname{Im}[\ ]$  are the real and imaginary parts respectively.

The Gaussian curvature is defined as the product of the two principal curvatures [23] and can be written as

$$K = \frac{-4 |P' Q - P Q'|^2}{(|P|^2 + |Q|^2)^4} \quad (7)$$

Where  $P' = \frac{dP}{d\rho}$  and  $Q' = \frac{dQ}{d\rho}$ .

The same parameters for equations (2) are the following:

$$g_{11} = g_{22} = |R(\omega)|^2 (1 + |\omega|^2)^2 \quad (8)$$

$$\vec{N} = \frac{1}{|\omega|^2 + 1} [2 \operatorname{Re}[\omega], 2 \operatorname{Im}[\omega], |\omega|^2 - 1] \quad (9)$$

$$K = \frac{-4}{|R(\omega)|^2 (1 + |\omega|^2)^4} \quad (10)$$

Finally, for equations (3) we have

$$g_{11} = g_{22} = \frac{|F|^2 (1 + |G|^2)^2}{4} \quad (11)$$

$$\vec{N} = \frac{1}{|G|^2 + 1} [2 \operatorname{Re}[G], 2 \operatorname{Im}[G], |G|^2 - 1] \quad (12)$$

$$K = - \left[ \frac{4 |G'|}{|F| (1 + |G|^2)^2} \right]^2 \text{ where } G' = \frac{dG}{dr} \quad (13)$$

Note that the Gaussian curvature "K" is always negative or zero this means that each point of the surface is a saddle point if "K < 0" (hyperbolic point), and a flat point when "K = 0" [5].

The Weierstrass equations have been written in different forms because in some cases, depending on the Weierstrass functions, the integration is easier if we use a particular form. In the following sections we compute some MS using the forms given in equations (2) and (3).

### 3 Computation of Minimal Surfaces

#### 3.1 Family of Enneper's Surfaces

For the Enneper's surfaces, Weierstrass equations in the form of eq. (3) are used. The Weierstrass functions for these surfaces are  $F = 1$  and  $G = \tau^k$  where "k" is the order of the surface [8]. After integrating from zero to  $\tau_0$  using the fact that these contour integrals are independent of the path ( $\vec{r}(u, v)$  is an harmonic function), we obtain the following values for the Cartesian coordinates  $(x, y, z)$ .

$$\begin{aligned} x &= \frac{1}{2} \left[ r \cos \phi - \frac{r^{2k+1}}{2k+1} \cos[(2k+1)\phi] \right] \\ y &= \frac{-1}{2} \left[ r \sin \phi - \frac{r^{2k+1}}{2k+1} \sin[(2k+1)\phi] \right] \\ z &= \frac{r^{k+1}}{k+1} \cos[(k+1)\phi] \end{aligned} \quad (14)$$

Where we have expressed the complex number  $\tau_0$  as  $\tau_0 = r e^{i\phi}$ .

In order to construct the surface we have to evaluate  $x, y$  and  $z$  for different values of  $\tau_0$ . In this case the integration domain that has been chosen consists in all the points inside a circle of radius 1 in the complex plane. These points constitute the values of  $\tau_0$  that we need to get several coordinates  $x, y$  and  $z$  in Cartesian 3-space. In figure 1 the Enneper's surfaces for  $k = 1, k = 2, k = 3$  and  $k = 4$  are shown.

#### 3.2 Family of one Planar Limit Minimal Surfaces

The Weierstrass functions to construct the family of one planar end minimal surfaces of order "k" [8] are given by :

$$F = \tau^{-2} \quad \text{and} \quad G = \tau^{k+1}$$

After Integrating these functions using equations (3) without including  $\tau = 0$  (singular point), we obtain the following coordinates  $x, y, z$  in real space

$$\begin{aligned} x &= \frac{1}{2} \left[ -\frac{\cos \phi}{r} - \frac{r^{2k+1}}{2k+1} \cos(2k+1)\phi \right] \\ y &= \frac{1}{2} \left[ -\frac{\sin \phi}{r} - \frac{r^{2k+1}}{2k+1} \sin(2k+1)\phi \right] \\ z &= \frac{r^k \cos k\phi}{k} \end{aligned}$$

Giving values of  $r$  between .1 and one, and values of  $\phi$  between zero and  $2\pi$  with  $k = 1$  we get the surface shown in fig. 2. Note that, again, we have put a complex number  $\tau_0$  as  $r e^{i\phi}$ .

#### 3.3 Scherk's Saddles and Associated Minimal Surfaces

The Scherk's Saddles are obtained if

$$F(\tau) = \frac{1}{t^{2(k+1)} + 1} \quad \text{and} \quad G(\tau) = \tau^k$$

The Contour integrals for these values of  $F$  and  $G$  can be solved analytically. Considering the same integration domain as in the Enneper's family (the points inside a circle of radius 1 in the complex plane), the surfaces of figure 3. are obtained.

Let us examine an interesting transformation called the Bonnet transformation which allow us to twist a MS preserving the metric (the arc-length between two points remains the same) and the Gaussian curvature. The transformation consists in multiplying the integrand of the Weierstrass equations by  $e^{i\theta}$ , if  $\theta = 90^\circ$  the surface is called adjoint. The Bonnet related surfaces are called associate. Basically, the importance of the Bonnet transformation resides in that the associate surfaces are also minimal surfaces, therefore, can be used to generate new minimal surfaces [10]. An example of this are the Gyroid (G-surface) and the  $P$  surfaces which are associates of the D-surface [2] (see TPMS section).

In particular, the Scherk's saddle with  $k = 1$  can be used as a fundamental element to construct a singly periodic minimal surface (MS periodic in one direction), and by applying the Bonnet transformation on this element with  $\theta = 90^\circ$ , a doubly periodic MS is obtained (MS periodic in two directions) (see fig. 4a and 4c). On the other hand, with the adjoint surface of the Scherk's  $k=2$  it is possible to build up an hexagonal layer (see figures 4b and 4d).

### 3.4 The Catenoid and the Helicoid

For the catenoid  $F = 1$ ,  $G = 1/\tau$ , and for the helicoid  $F = 1$ ,  $G = i/\tau$ . These two MS are related by the Bonnet Transformation where  $\theta = 90^\circ$ , this means that the helicoid is the adjoint of the catenoid. (see fig. 5). Note that the function  $G$  has a singular point at  $\tau = 0$  (origin of the complex plane), therefore, this point must not be considered in the integration domain.

## 4 Triply Periodic Minimal Surfaces

An algorithm for constructing Triply Periodic Minimal Surfaces (TPMS) has been developed by Lidin and Hyde [11] in which the normals to the flat points of the surface (points where the Gaussian curvature is zero) are used to build up the Weierstrass function  $R(\omega)$  ( see eq.(2) ). According to this algorithm  $R(\omega)$  is given by

$$R(\omega) = \prod_{\alpha=0}^{\pi} (\omega - \omega_{\alpha})^{-1/b} \quad (15)$$

Where  $\omega_{\alpha}$  are the images of the flat points on the surface in the complex plane. These values of  $\omega_{\alpha}$  are obtained via stereographic projection of the normals to the flat points. The value of  $b$  depends on the topology of the surface [6]. Some of the Weierstrass polynomials reported in the literature have been collected here .

The procedure for obtaining TPMS consists basically in two steps. First, in computing the Weierstrass equations in order to generate the Cartesian coordinates  $x, y, z$  of a fundamental element of the surface, and second, in applying symmetry operations to this element for constructing the hole surface. Regarding the Weierstrass integrals (elliptic integrals), An integration algorithm is needed, like for example , a Simpsons's rule or a mid-point rule [19]. The integration should be carried out for points inside an adequate integration domain avoiding singular points, although in some cases, important parts of the surface reside very close to the singularities. It is important to remember that the integrals are independent of the path in a regular region. For drawing the fundamental element, a mesh of points inside the integration domain can be generated to get different values of  $x, y, z$ , so that the points in Cartesian space which compose the surface are joined in the same order as the mesh points in the complex plane (inside the integration domain).

### 4.1 D, G and P Triply Periodic Minimal Surfaces

The Weierstrass function for the fundamental element of the D-Surface (diamond surface)

is  $R(\omega) = (\omega^8 - 14\omega^4 + 1)^{-1/2}$  [16],[2] with an integration domain given by the points around the origin limited by 4 circles with radius  $\sqrt{2}$  and centres at  $(\pm/\sqrt{2}, \pm i/\sqrt{2})$  (see figures 6 and 7). The G-surface or gyroid ( discovered by Alan Schoen [21]) and the P-surface (primitive surface) are related to the D-surface by Bonnet transformation: the Bonnet angle for the G-surface is  $38.015^\circ$  and for the P-surface is  $90^\circ$ .

## 4.2 The H-Surface or Hexagonal TPMS

Another example of a TPMS is the H-surface (Hexagonal) for which the Weierstrass function is

$$R(\omega) = [\omega^8 - \omega^6(F_1 - F_2 - 1) + \omega^4(F_3 - F_2 F_1 - F_1 + F_2) - \omega^2(F_2 F_3 + F_3 - F_1 F_2) + 1]^{-\frac{1}{2}}$$

Where

$$F_1 = \frac{6 - 14E^2}{(2 + \sqrt{1 - E^2})^2}$$

$$F_2 = \frac{E^2}{(1 - \sqrt{1 - E^2})^2}$$

$$F_3 = \frac{(3 + E^2)^2}{(2 + \sqrt{1 - E^2})^4} \text{ and } 0 < E < 1$$

The integration domain consists in the region surrounding the origin bounded by the two circles of radius  $\sqrt{4/3}$  and centres at  $(0, \pm i/\sqrt{1/3})$  (see fig. 8). The values of  $\omega_\alpha$  (see eq.(15)) for the H-surface are:  $\pm 1, \pm E/(1 - \sqrt{1 - E^2})$  and  $(\pm E \pm i\sqrt{3}/2\sqrt{1 - E^2})/(1 + 1/2\sqrt{1 - E^2})$ . The parameter "E" is related to the "c/a" ratio of the fundamental element.

## 4.3 Other Weierstrass Functions

### T-surface (Tetragonal Surface)

$$R(\omega) = [\omega^8 - \frac{(16(1 - A^2) + 2A^4)}{A^4} \omega^4 + 1]^{-\frac{1}{2}} \quad 0 < A < 1$$

Where the values of  $\omega_\alpha$  (see eq. 15) are  $\pm A/(1 \pm \sqrt{1 - A^2})$  and  $iA/(1 \pm \sqrt{1 - A^2})$ . These values which correspond to the stereographic projection of the flat points onto the complex plane are plotted in fig. 9. The D-Surface and the Scherk  $k = 1$  surfaces are a special case of the T-surface. Changing "A" the "c/a" ratio changes too [11].

### CLP-Surface

$$R(\omega) = [\omega^8 - (16(A^4 - A^2) + 2)\omega^4 + 1]^{-\frac{1}{2}}$$

where  $0 < A < \frac{1}{\sqrt{2}}$  and with flat point images  $\omega_\alpha$  at  $\pm A \pm i\sqrt{1 - A^2}$  and  $\pm\sqrt{1 - A^2} \pm iA$ . The stereographic projection of the flat points onto the complex plane is shown in fig. 10. As in the T-surface, the parameter "A" is related to the "c/a" ratio of the surface fundamental element [11].

### I-WP Surface

The Weierstrass function  $R(\omega)$  for the I-WP surface has been published recently [12] and is given by

$$R(\omega) = [\omega^6 - 5\omega^4 - 5\omega^2 + 1]^{-\frac{2}{3}}$$

The function above is obtained using equation (15) with  $\omega_\alpha = \pm i, \pm\sqrt{2} \pm 1$ . The stereographic projection of the fundamental element of the surface onto the complex plane is shown in fig. 10.

## 5 Conclusion

Has been shown that the use of the Weierstrass equations is convenient for computing minimal surfaces since, on one hand, these equations guarantee that the surface has zero mean curvature and on the other hand, knowing the Weierstrass functions we can calculate important parameters for characterising the surface (the metric, the normal vectors and the Gaussian curvature). In addition, the Weierstrass parametrization allow us to apply the Bonnet transformation for generating a variety of minimal surfaces preserving the metric and the Gaussian curvature. Perhaps a weak point of the Weierstrass equations in the computation of minimal surfaces is that in some surfaces, in particular TPMS, we have to integrate very close to the singularities because important parts of the surface reside very near to these points. Finally, the Weierstrass equations should be considered as a method for finding new minimal surfaces which can be important to describe properties in biological or inorganic systems.

## References

- [1] Anderson D.M. and Ström P.; Polym. Assoc. Struct., ACS Symposium Series No.384, M.A. El-Nokaly Ed. Amer. Chem. Soc., (1989).
- [2] Andersson S., Hyde S.T., Larsson K., Lidin S., Chem. Rev., **88**, 221-242, (1988).
- [3] Boas M.L., "Mathematical Methods in the Physical Sciences", John Wiley and Sons, Inc. (1966).
- [4] Douglas J., Trans. Amer. Math. Soc., **33**, (1931).
- [5] Hilbert D., and Cohn-Vossen S., "Geometry and Imagination", Chelsea Publishing Company, (1952).
- [6] Hyde S.T., Z. Kristallogr., **187**, 165-185, (1989).
- [7] Hyde S.T. and Andersson S., Z. Kristallogr., **174**, 237-245, (1986).
- [8] Karcher H., "Construction of Minimal Surfaces", Vorlesungsreihe No. 12, Institut für Angewandte Mathematik der Universität Bonn, (1989).
- [9] Kreyszig E., "Differential Geometry", University of Toronto Press, (1959).
- [10] Lidin S., J. Chem. Soc. Faraday Trans., **86**, 769-775, (1990).
- [11] Lidin S., and Hyde S.T., J. Phys. France, **48**, 1585-1590, (1987).
- [12] Lidin S., Hyde S.T., Ninham B.W., J.Phys. France, **51**, 801-813, (1990).
- [13] Mackay A.L., IUC Copenhagen Meeting, poster, (1979).
- [14] Mackay A.L., Physica **131 B**, 300-305, (1985).
- [15] Maxwell, J.C. and Rayleigh, Lord, Capillary Action, "Encyclopedia Britanica", 13th ed., Vol. 5, pp.256-275.
- [16] Nitsche, J.C.C., "Lectures on Minimal Surfaces", Vol. 1, Cambridge University Press, (1989).
- [17] Plateau J.A.F., Statique Expérimentale et Théorique des Liquides Soumis aux Seules Forces Moléculaires (Gauthier-Villars, Trubner et Cie, F. Clemm), 2 Vols.,(1873).

- [18] Porter A.W., Surface Tension, "Encyclopedia Britannica", **21**, 595, (1964).
- [19] Press W.H., Flannery B.P., Teukolsky S.A., Vetterling W.T., "Numerical Recipes", Cambridge University Press, (1986).
- [20] Rado T., Math. Zeit., vol.2, (1930).
- [21] Schoen A.H., NASA Technical Note **TN D-5541**, "Infinite Periodic Minimal Surfaces Without Self-Intersections", Electronics Research Center Cambridge, Mass. 02139, (1970).
- [22] Scriven L.E., Nature (London), **266**, 123, (1976).
- [23] Struik D.J., "Differential Geometry", Addison-Wesley, (1961).
- [24] Weierstrass K., "Untersuchungen über die Flächen, deren mittlere Krümmung überall gleich Null ist", Monatsber. d. Berliner Akad. 612-625, (1866).

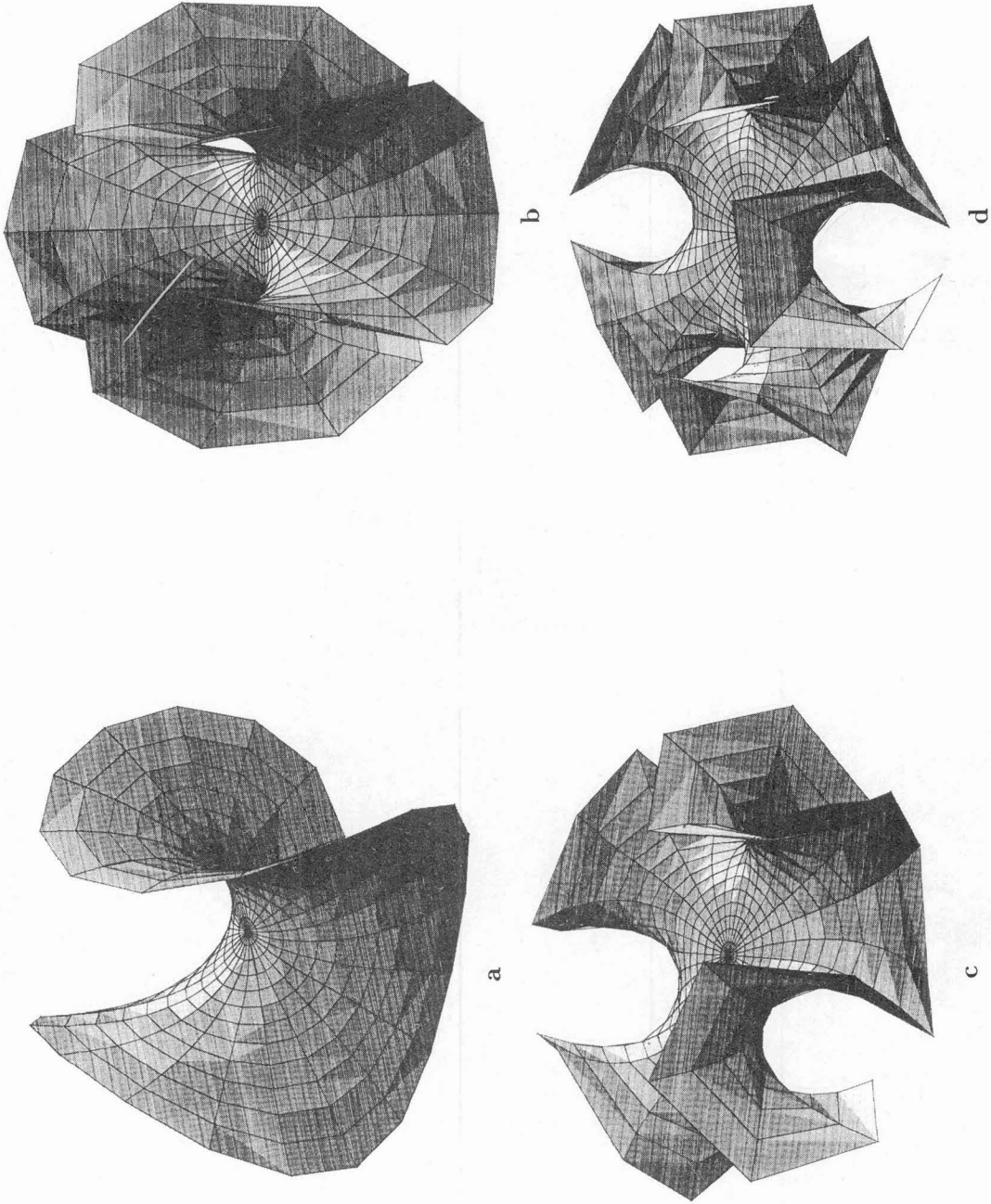


Figure 1

Figure 1.- Family of Enneper's Surfaces with (a)  $k=1$ , (b)  $k=2$ , (c)  $k=3$ , (d)  $k=4$ .

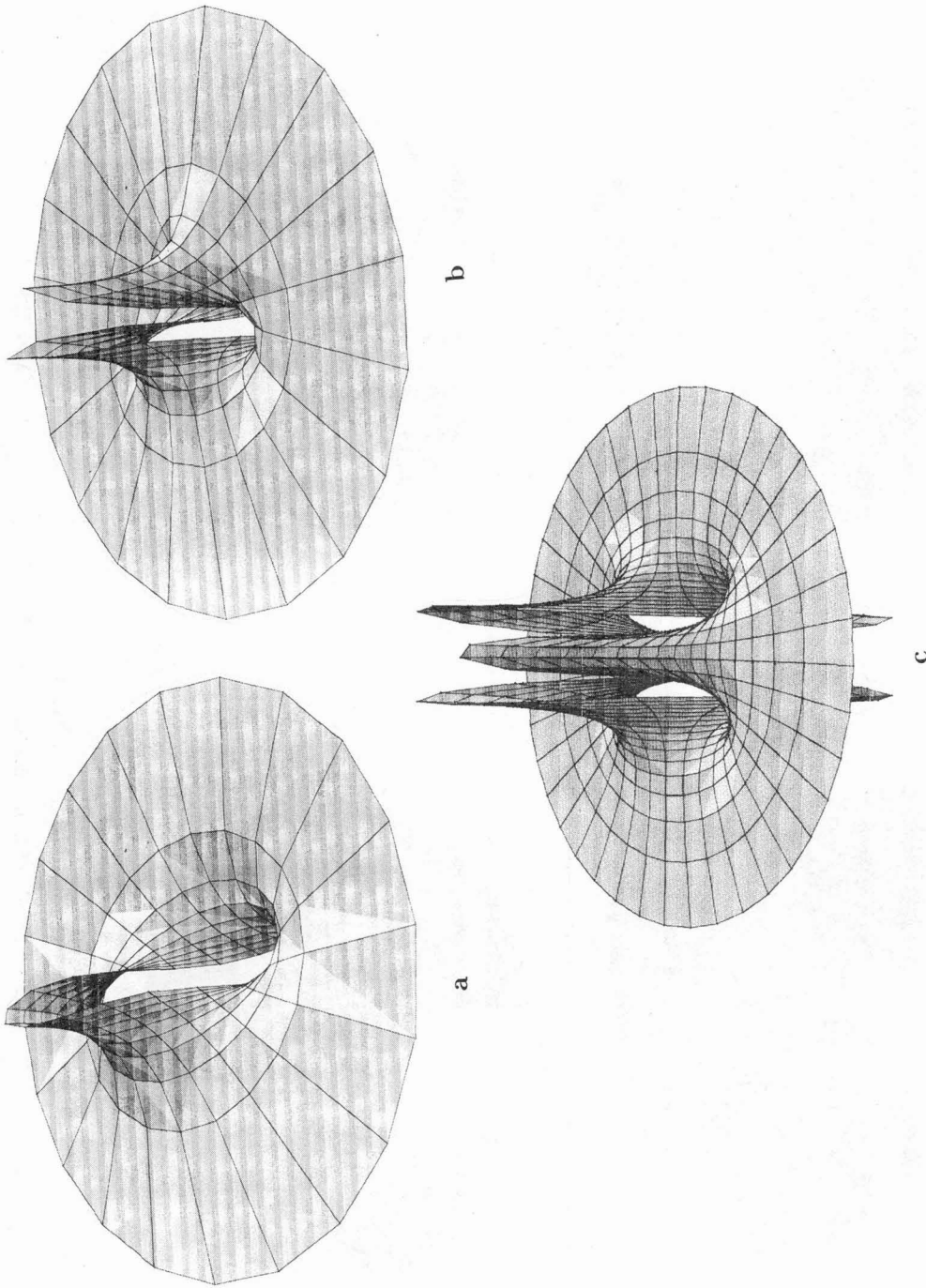
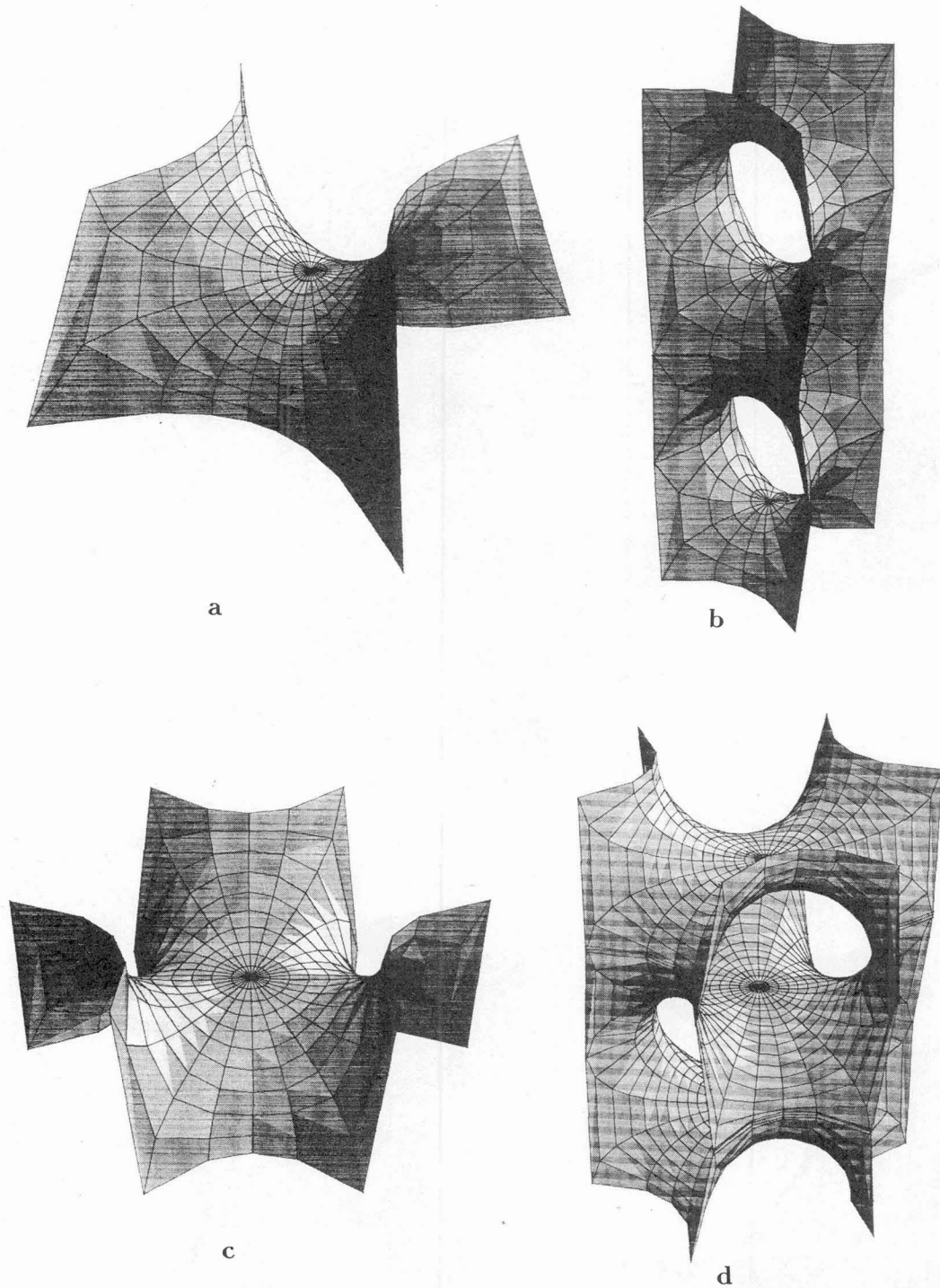


Figure 2

Figure 2.- One planar end minimal surfaces with (a)  $k=1$ , (b)  $k=2$ , and (c)  $k=3$ .



**Figure 3**

Figure 3.- (a) Scherk's minimal surface with  $k=1$ . (b) Scherk's saddle Tower with  $k=1$ .  
(c) Scherk's minimal surface with  $k=2$ .  
(d) Scherk's Tower with  $k=2$ .

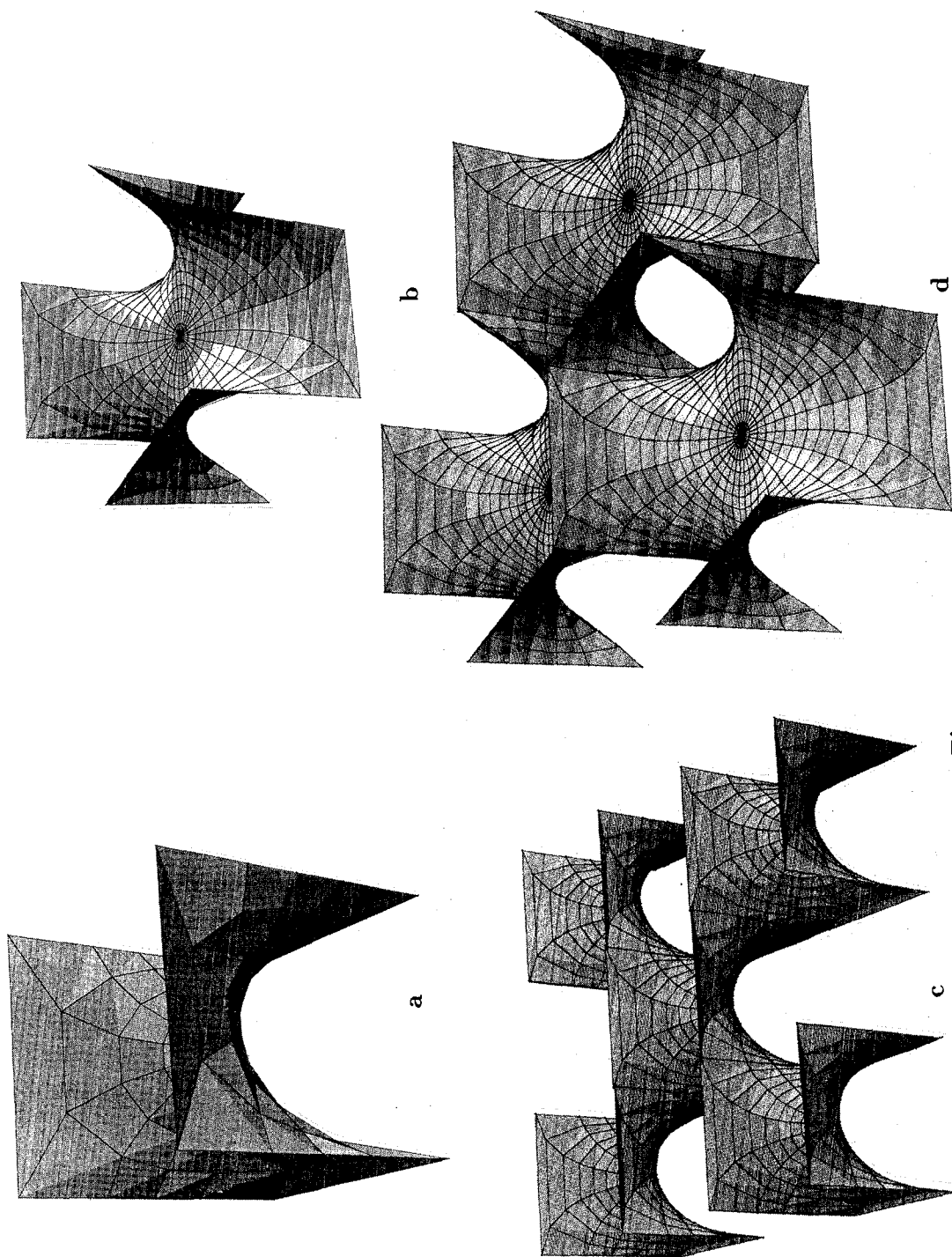
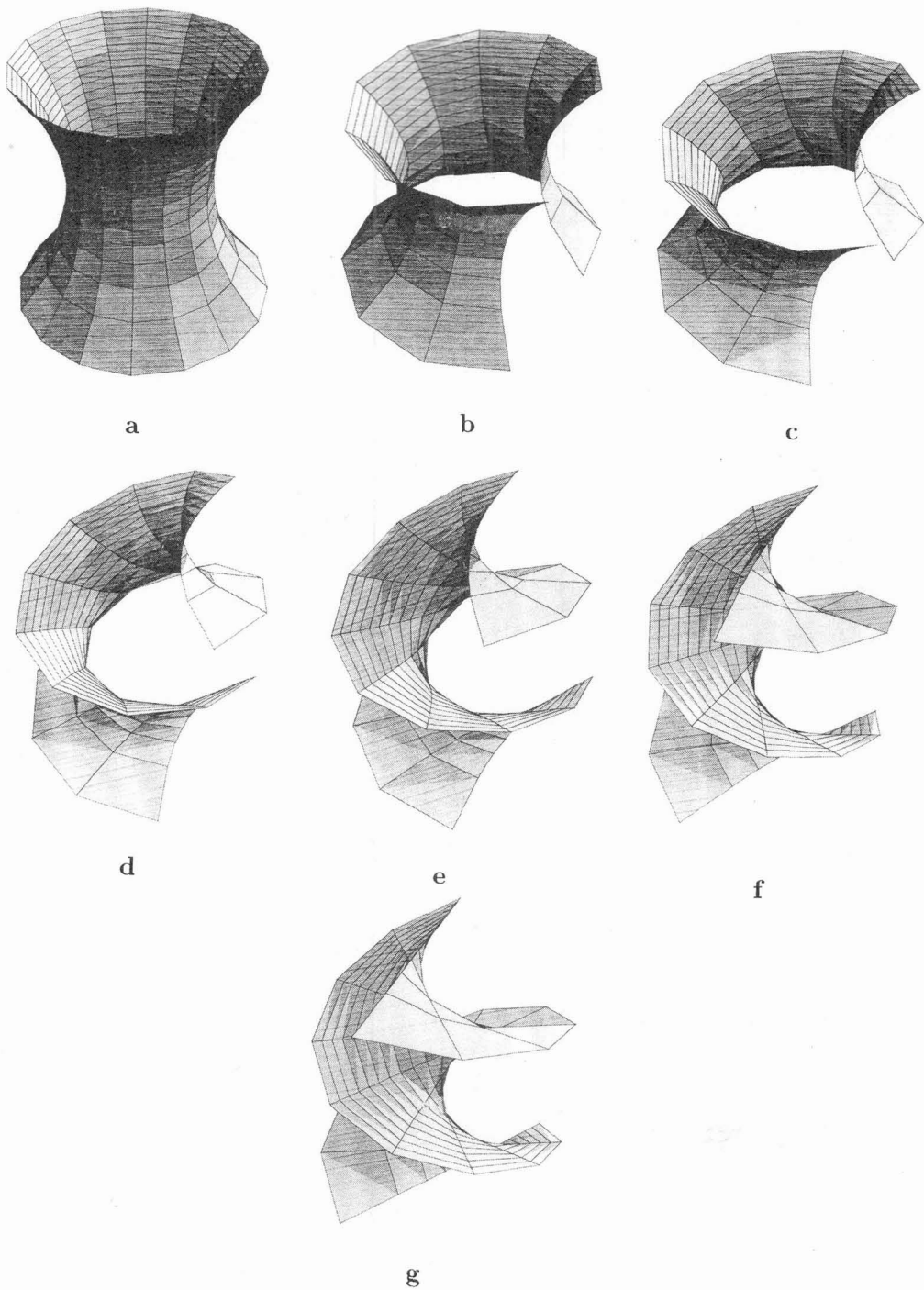
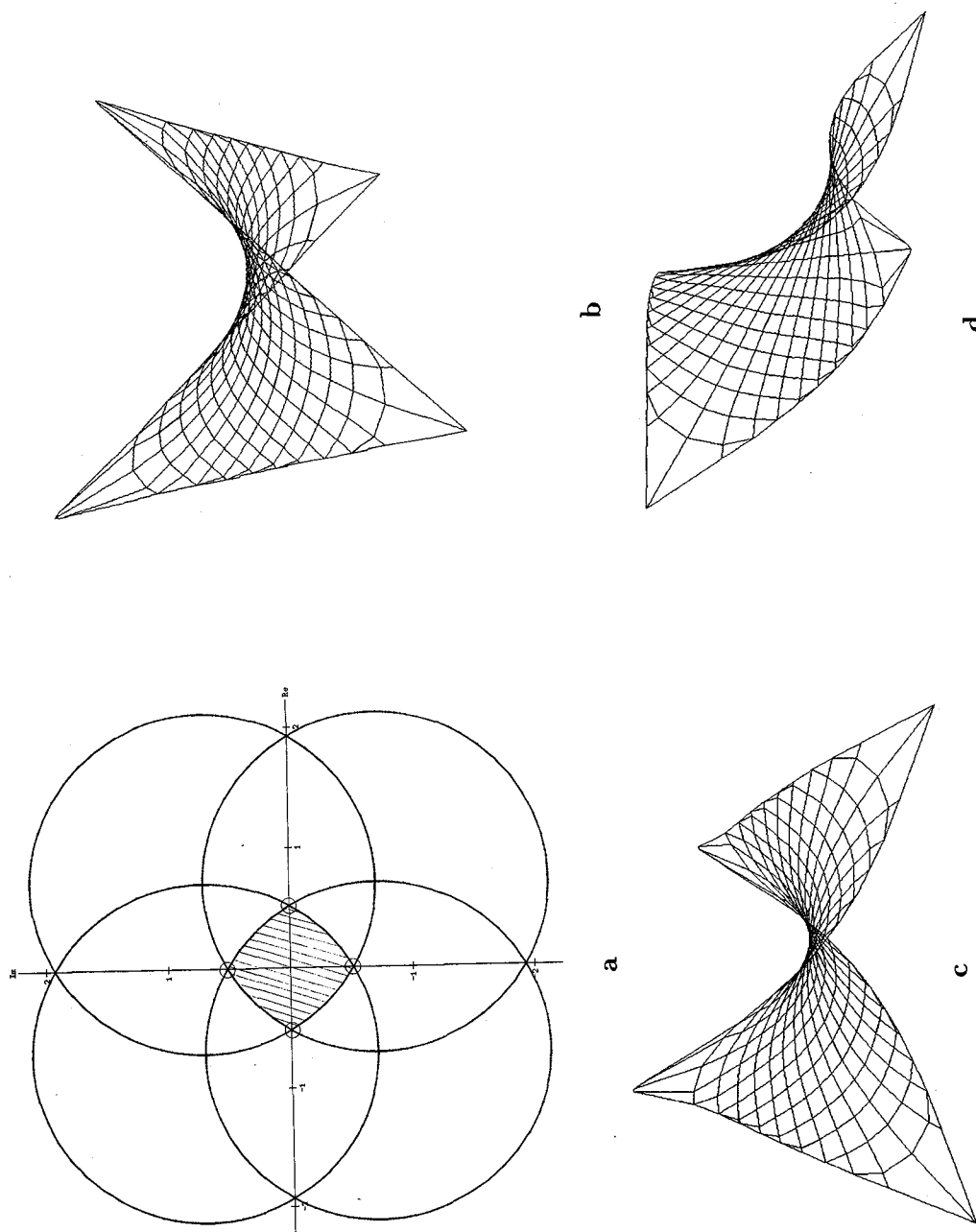
**Figure 4**

Figure 4.- (a) Adjoint of the Scherk's  $k=1$ . (b) Adjoint of the Scherk's  $k=2$ , obtained by the Bonnet transformation with  $\theta = 90^\circ$ . (c) Doubly periodic minimal surface constructed with the elements in (a). (d) Hexagonal layer constructed with the elements in (b).



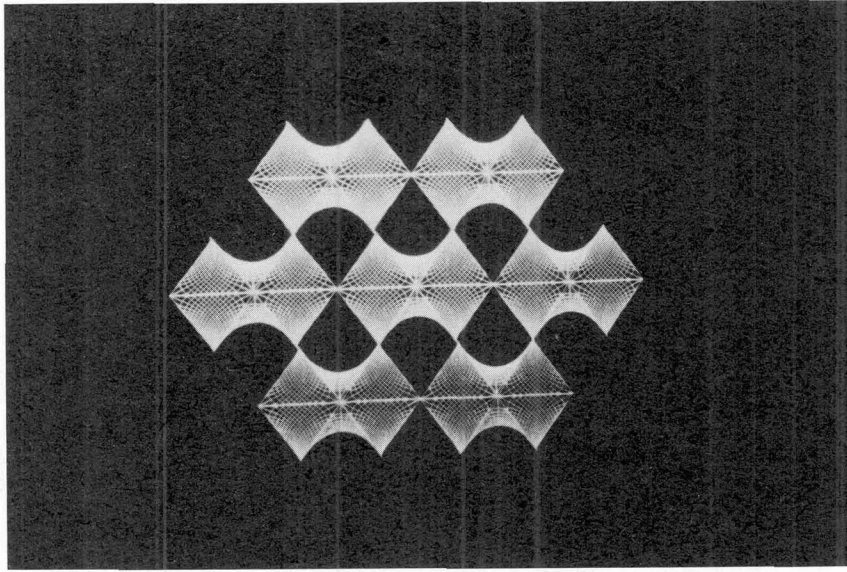
**Figure 5**

Figure 5.- Bonnet transformation of the catenoid into the helicoid (a)  $\theta = 0^\circ$ . (b)  $\theta = 10^\circ$ . (c)  $\theta = 20^\circ$ . (d)  $\theta = 40^\circ$ . (e)  $\theta = 60^\circ$ . (f)  $\theta = 80^\circ$ . (g)  $\theta = 90^\circ$ .

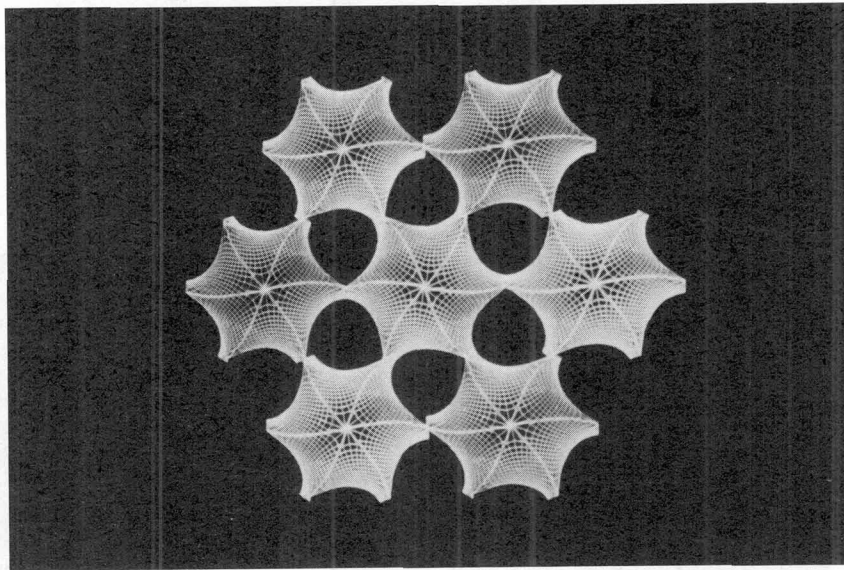


**Figure 6**

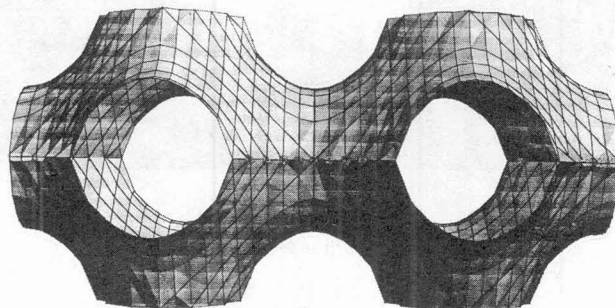
Figure 6.- (a) Integration domain for the D, G and P surfaces. (b) Fundamental element of the D-surface ( $\theta = 0^\circ$ ). (c) Fundamental element of the G-surface ( $\theta = 38.015^\circ$ ). (d) Fundamental element of the P-surface ( $\theta = 90^\circ$ ).



a



b



c

**Figure 7**

Figure 7.- (a) D-surface. (b) G-surface or Gyroid. (c) P-surface.

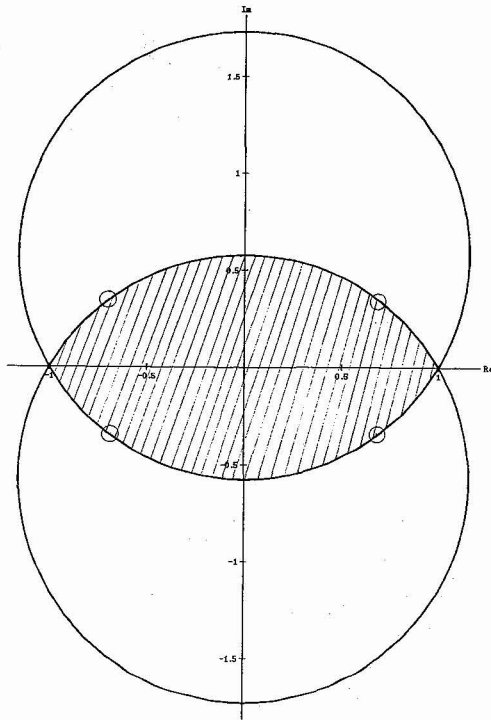
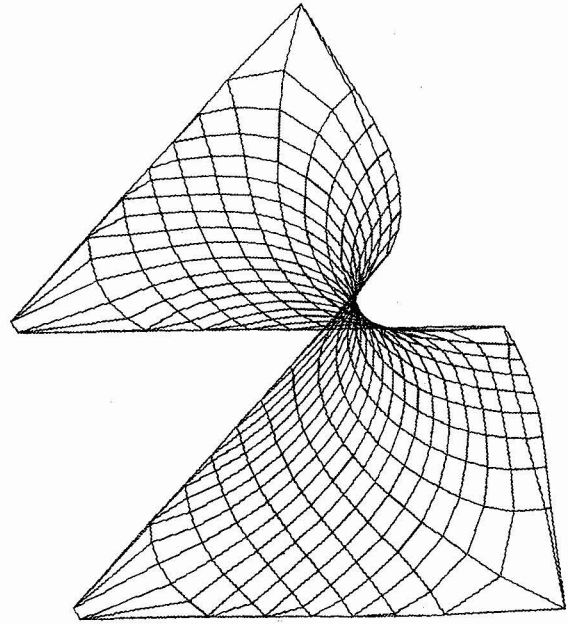
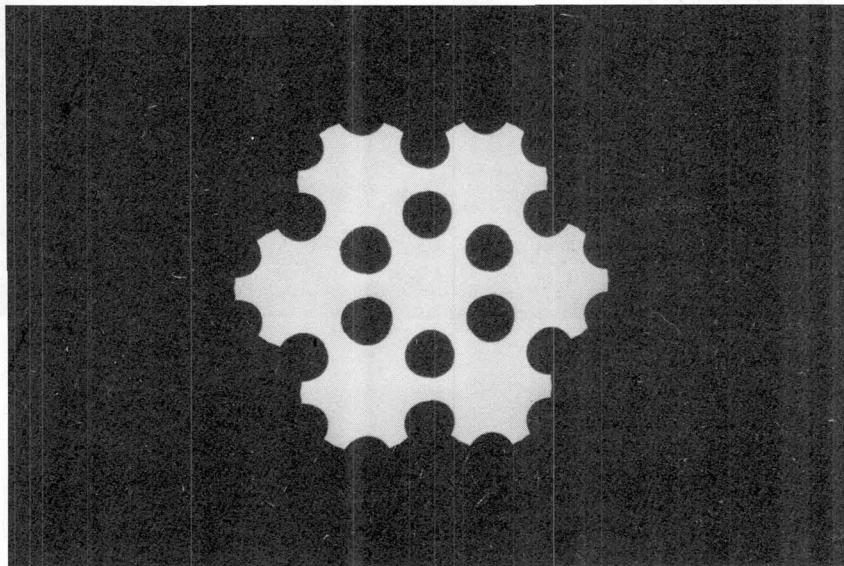
**a****b****c****Figure 8**

Figure 8.- (a) Integration domain of the H-surface. (b) Fundamental element of the H-surface. (c) The H-surface.

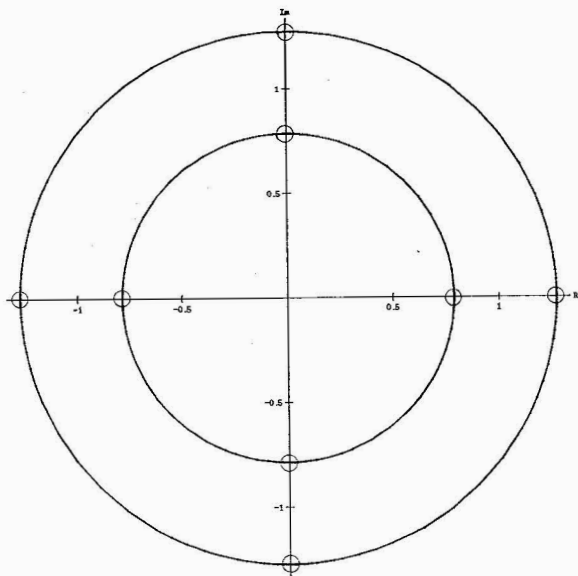
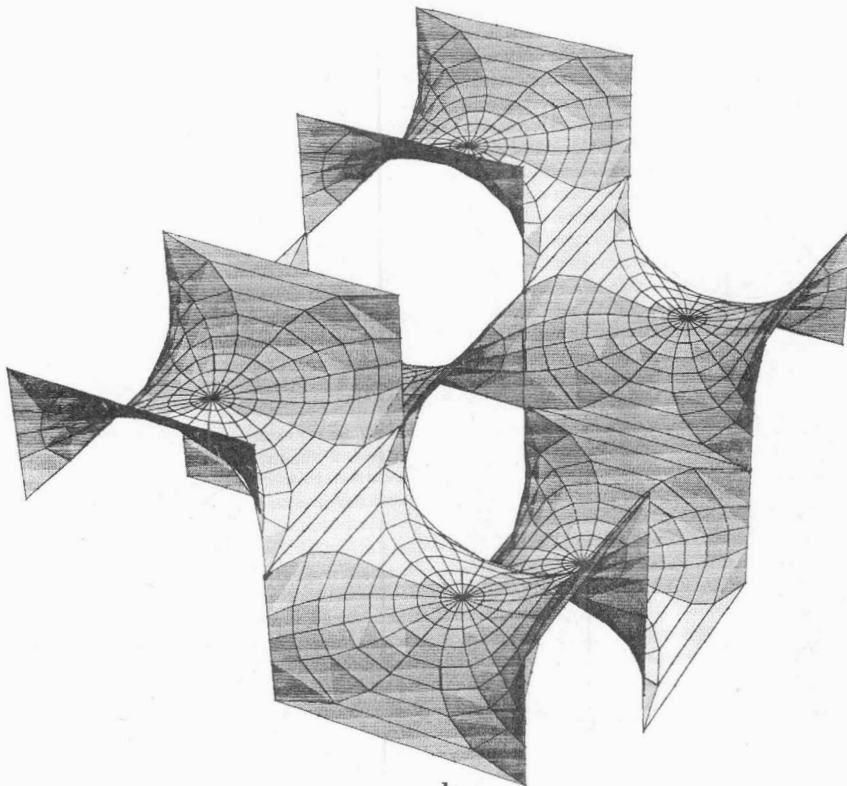
**a****b****Figure 9**

Figure 9.- (a) Images of the flat points of the T-surface onto the complex plane. (b) The T-surface.

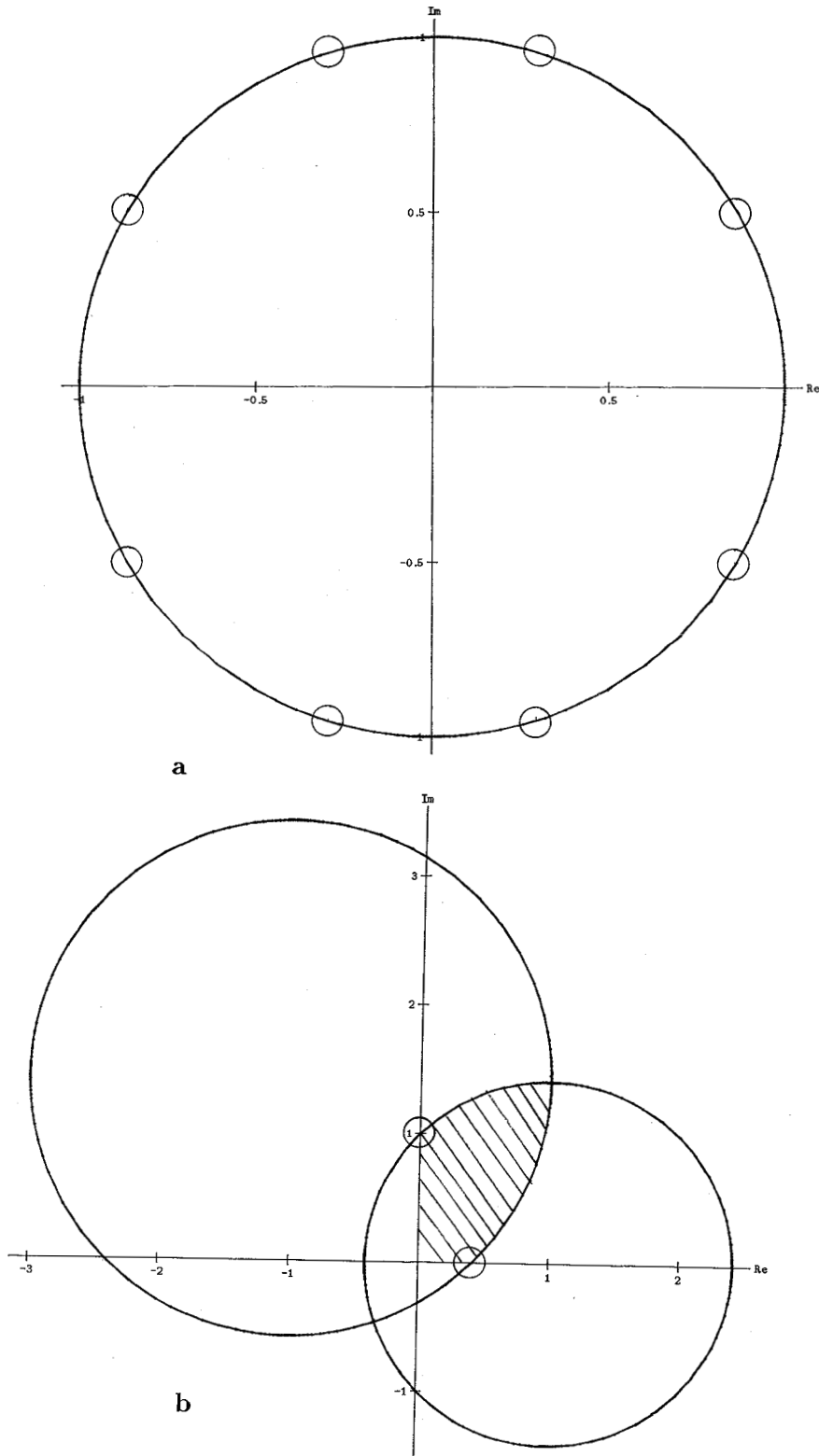
**Figure 10**

Figure 10.- (a) Images of the flat points of the CLP-surface onto the complex plane.  
(b) Fundamental element of the I-WP surface onto the complex plane.